

GCA Technical Report No. 65-15-N

PHYSICS OF PLANETARY ATMOSPHERES II:
THE FLUORESCENCE OF SOLAR IONIZING RADIATION

A. Palgarno
M.B. McElroy

GCA CORPORATION
GCA TECHNOLOGY DIVISION
Bedford, Massachusetts

Contract No. NASW-1283

Prepared for
NATIONAL AERONAUTICS AND SPACE ADMINISTRATION
HEADQUARTERS
Washington, D. C.

May 1965

N65-31047

(ACCESSION NUMBER)	(THRU)
45	1
(PAGES)	(CODE)
CR 64424	29
(NASA CR OR TMX OR AD NUMBER)	(CATEGORY)

FORM 602

TABLE OF CONTENTS

<u>Section</u>	<u>Title</u>	<u>Page</u>
1	INTRODUCTION	1
2	ION PRODUCTION RATES	1
3	EXCITATION REMOVAL PROCESSES	9
	3.1 Atomic Oxygen Ions	9
	3.2 Molecular Nitrogen Ions	10
	3.3 Molecular Oxygen Ions	14
4	OTHER EXCITATION MECHANISMS	21
	REFERENCES	23

PHYSICS OF PLANETARY ATMOSPHERES II:

THE FLUORESCENCE OF SOLAR IONIZING RADIATION

by A. Dalgarno and M.B. McElroy[†]

ABSTRACT

The mid-day dayglow intensities arising from the fluorescence of solar ionizing radiation are calculated. The predicted overhead intensities above 120 km of the $O^+(2P-2D)$ lines at $\lambda\lambda 7319-7330\text{\AA}$, the Meinel band system of N_2^+ , the first negative system of N_2^+ , the first negative system of O_2^+ , the Höpfield emission system of O_2^+ and the second negative system of O_2^+ are, respectively, 500 R - 1 kR, 9 kR, 600 R, 2 kR, 600 R and 400 R.

31047

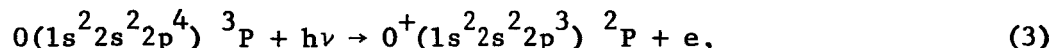
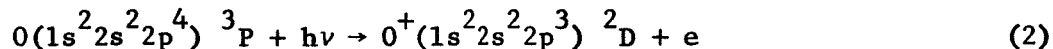
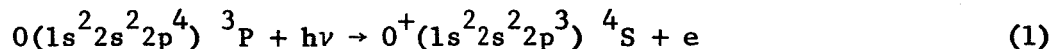
Author

1. INTRODUCTION

When solar ultraviolet radiation ionizes an atmospheric constituent, the positive ion may be left in an excited electronic level which can radiate. The fluorescent emission may be detectable using rocket-borne or ground-level instrumentation, thereby providing an optical method for the investigation of the ionosphere. In particular, it may be possible to monitor the solar ionizing radiations by observations in the visible [1].*

2. ION PRODUCTION RATES

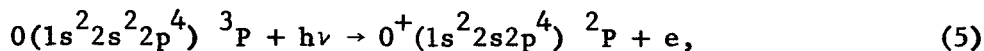
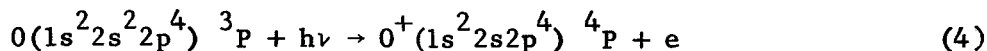
The absorption of ionizing radiation by atomic oxygen can lead to a significant population of several excited states of the resulting positive ion. Thus the ejection of an outer shell electron from atomic oxygen proceeds according to



[†] Kitt Peak National Observatory, Tucson, Arizona, U. S. A.

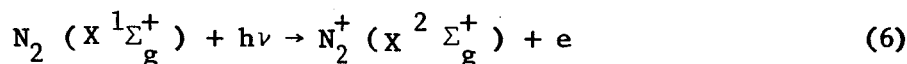
* Numbers in [] throughout the text represent reference numbers.

the spectral heads of which are located at, respectively, 910Å, 732Å, and 663Å. The ejection of an inner shell electron from atomic oxygen proceeds according to

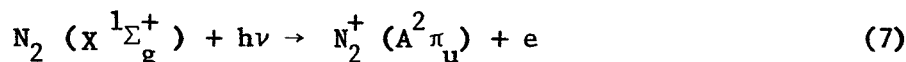


the spectral heads of which are located at, respectively, 434Å and 310Å.

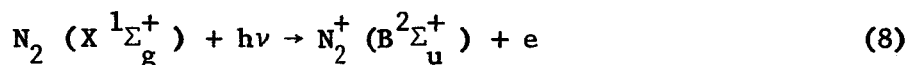
The configuration of molecular nitrogen in the ground state is $(KK \sigma_g 2s^2 \sigma_u 2s^2 \pi_u 2p^2 \sigma_g 2p^2) {}^1\Sigma_g^+$. The first ionization potential of N_2 is equivalent in energy to a wavelength of 796Å, corresponding to the transition



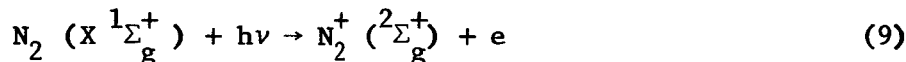
in which a $\sigma_g 2p$ electron is ejected. At 732Å, a $\pi_u 2p$ electron can be ejected, corresponding to the transition



and at 661Å a $\sigma_u 2s$ electron can be ejected, corresponding to the transition

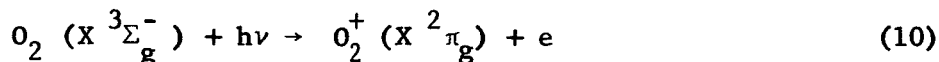


The location of the spectral head for the ejection of a $\sigma_g 2s$ electron corresponding to

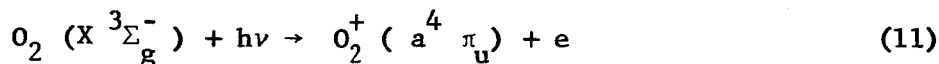


is uncertain and we have assumed arbitrarily that it is 350Å.

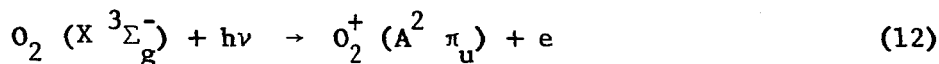
The configuration of molecular oxygen in the ground state is $(KK \sigma_g 2s^2 \sigma_u 2s^2 \sigma_g 2p^2 \pi_u 2p^4 \pi_g 2p^2) {}^3\Sigma_g^-$. At 1026Å, a $\pi_g 2p$ electron can be ejected corresponding to



At 767Å, a $\pi_u 2p$ electron can be ejected corresponding to

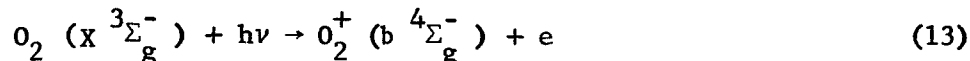


and at 729Å, a $\pi_u 2p$ electron corresponding to

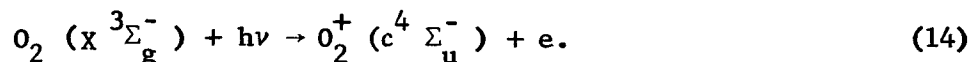


A $\sigma_g 2p$ electron can be ejected by radiation shorter than perhaps 682Å

corresponding to



and a $\sigma_u 2s$ electron by radiation shorter than 504\AA corresponding to



There are other discontinuities in the photoionization cross section yielding O_2^+ in unidentified doublet and quartet Σ_u and Σ_g states. We have assumed arbitrarily that the $^4\Sigma$ states are energetically accessible to radiation shorter than 430\AA and the $^2\Sigma$ states to radiation shorter than 310\AA .

The photoionization cross sections for the individual transitions are available for atomic oxygen from theoretical calculations [2]. For molecular oxygen and molecular nitrogen we have assumed, following earlier work [3], that whenever the photon energy is such that a multiplicity of ionizing transitions can occur the probability of a particular transition is proportional to the statistical weight of the product positive ion states and we have employed the measured total cross sections of Huffman, Tanaka and Larrabee [4], Cook, Ching and Becker [5], and Samson and Cairns [6]. Schoen [7] has recently given estimates of the percentages of photoionizing transitions in molecular oxygen and nitrogen which terminate in particular states. His estimates are uncertain but they suggest that for N_2^+ the production rate of the $\text{A}^2\Pi_u$ state should be increased by 50% and the production rate of the $\text{B}^2\Sigma_u^+$ state should be decreased by 75%, the production rate of the ground state being altered so that no change in the total N_2^+ production rate occurs. They suggest that for O_2^+ the production rates of the $\text{a}^4\Pi_u$ and $\text{A}^2\Pi_u$ states should be decreased by 50% and the production rate of the $\text{b}^4\Sigma_g^-$ state should be increased by 100%, the production rate of the ground state being altered so that no change in the total O_2^+ production rate occurs. We have made these changes consistently throughout the calculations.

For the distribution of neutral particles we have used the analytical representations introduced by Bates [8] and tabulated by McElroy [9]. Our calculations refer to the model atmosphere with an exospheric temperature of 750°K , a temperature gradient of 20°K km^{-1} at an altitude of 120 km and the particle distributions listed in Table 1. This atmosphere is in harmony with that derived by Hinteregger, Hall and Schmidtke [10] from an analysis of solar ultraviolet absorption (cf. McElroy[11]). For the incident flux of solar photons we have used values reported by Hinteregger [12], Hinteregger, Hall and Schmidtke[10], Hall, Schweizer and Hinteregger [13], and Hall, Schweizer, Heroux and Hinteregger[14]. The resulting ion production rates are presented in Tables 2, 3 and 4.

TABLE 1
ATMOSPHERIC NUMBER DENSITIES CM^{-3}

Altitude (km)	n(O)	n(O ₂)	n(N ₂)	n(He)	n _e
650	1.79(5)	6.44(-1)	4.53(1)	4.35(5)	8.91(4)
600	5.08(5)	5.19	2.82(2)	5.64(5)	1.10(5)
550	1.46(6)	4.31(1)	1.80(3)	7.36(5)	1.51(5)
500	4.29(6)	3.69(2)	1.18(4)	9.63(5)	2.09(5)
450	1.27(7)	3.26(3)	7.94(4)	1.26(4)	2.88(5)
400	3.85(7)	2.98(4)	5.51(5)	1.67(6)	3.98(5)
350	1.18(8)	2.81(5)	3.93(6)	2.21(6)	5.25(5)
300	3.70(8)	2.74(6)	2.89(7)	2.94(6)	6.46(5)
275	6.58(8)	8.68(6)	7.92(7)	3.40(6)	6.57(5)
250	1.18(9)	2.78(7)	2.19(8)	3.93(6)	5.89(5)
225	2.12(9)	8.98(7)	6.12(8)	4.56(6)	4.68(5)
200	3.86(9)	2.96(8)	1.74(9)	5.33(6)	3.63(5)
190	4.94(9)	4.81(8)	2.67(9)	5.70(6)	3.31(5)
180	6.36(9)	7.91(8)	4.12(9)	6.12(6)	3.02(5)
170	8.29(9)	1.32(9)	6.47(9)	6.63(6)	2.88(5)
160	1.10(10)	2.26(9)	1.04(10)	7.28(6)	2.66(5)
150	1.51(10)	4.04(9)	1.74(10)	8.19(6)	2.54(5)
140	2.20(10)	7.83(9)	3.14(10)	9.64(6)	2.29(5)
130	3.62(10)	1.78(10)	6.59(10)	1.24(7)	2.00(5)
120	8.00(10)	6.00(10)	2.00(11)	2.00(7)	1.74(5)

TABLE 2
O⁺ PRODUCTION RATES CM⁻³

State Altitude(km)	² _D	² _P	⁴ _P	² _P
650	1.50(-2)	5.39(-3)	7.66(-5)	4.01(-5)
600	4.27(-2)	1.53(-2)	2.18(-4)	1.14(-4)
550	1.23(-1)	4.41(-2)	6.27(-4)	3.28(-4)
500	3.60(-1)	1.29(-1)	1.83(-3)	9.60(-4)
450	1.07	3.83(-1)	5.45(-3)	2.85(-3)
400	3.23	1.16	1.65(-2)	8.62(-3)
350	9.89	3.54	5.04(-2)	2.64(-2)
300	3.05(1)	1.09(1)	1.56(-1)	8.18(-2)
275	5.35(1)	1.92(1)	2.74(-1)	1.44(-1)
250	9.31(1)	3.33(1)	4.80(-1)	2.54(-1)
225	1.59(2)	5.68(1)	8.30(-1)	4.40(-1)
200	2.56(2)	9.19(1)	1.39	7.49(-1)
190	3.03(2)	1.09(2)	1.68	9.17(-1)
180	3.49(2)	1.25(2)	2.01	1.11
170	3.88(2)	1.40(2)	2.36	1.33
160	4.13(2)	1.49(2)	2.70	1.57
150	4.13(2)	1.50(2)	2.98	1.81
140	3.84(2)	1.41(2)	3.12	2.02
130	3.33(2)	1.24(2)	3.00	2.11
120	2.65(2)	9.92(1)	2.47	1.91

TABLE 3
 N_2^+ PRODUCTION RATES CM^{-2}

State Altitude(km)	$A^2_{\pi_u}$	$B^2_{\Sigma_u^+}$	$2_{\Sigma_g^+}$
650	1.29(-5)	9.43(-7)	6.72(-7)
600	8.04(-5)	5.85(-6)	4.18(-6)
550	5.13(-4)	3.75(-5)	2.67(-5)
500	3.36(-3)	2.45(-4)	1.75(-4)
450	2.26(-2)	1.65(-3)	1.18(-3)
400	1.57(-1)	1.14(-3)	8.16(-3)
350	1.11	8.12(-2)	5.80(-2)
300	8.09	5.87(-1)	4.23(-1)
275	2.17(1)	1.58	1.15
250	5.85(1)	4.25	3.12
225	1.53(2)	1.11(1)	8.40
200	3.78(2)	2.75(1)	2.22(1)
190	5.25(2)	3.80(1)	3.25(1)
180	7.06(2)	5.01(1)	4.71(1)
170	9.07(2)	6.62(1)	6.75(1)
160	1.09(3)	8.00(1)	9.54(1)
150	1.34(3)	8.88(1)	1.32(2)
140	1.15(3)	8.82(1)	1.79(2)
130	1.00(3)	8.08(1)	2.32(2)
120	9.66(2)	8.05(1)	2.82(2)

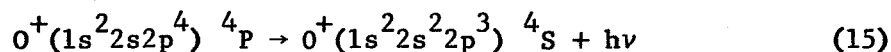
TABLE 4
 O_2^+ PRODUCTION RATES CM^{-3}

State Altitude(km)	$a^4\pi_u$	$A^2\pi_u$	$b^4\Sigma_g^-$	$c^4\Sigma_u^-$
650	7.25(-8)	3.46(-8)	1.27(-7)	3.17(-8)
600	5.80(-7)	2.79(-7)	1.03(-6)	2.56(-7)
550	4.84(-6)	2.31(-6)	8.54(-6)	2.12(-6)
500	4.14(-5)	1.98(-5)	7.30(-5)	1.82(-5)
450	3.66(-4)	1.75(-4)	6.46(-4)	1.61(-4)
400	3.34(-3)	1.60(-3)	5.88(-3)	1.47(-3)
350	3.14(-2)	1.50(-2)	5.54(-2)	1.38(-2)
300	3.02(-1)	1.45(-1)	5.34(-1)	1.33(-1)
275	9.45(-1)	4.51(-1)	1.66	4.16(-1)
250	2.92	1.40	5.16	1.30
225	8.90	4.26	1.57(1)	4.01
200	2.57(1)	1.23(1)	4.54(1)	1.20(1)
190	3.83(1)	1.83(1)	6.74(1)	1.83(1)
180	5.50(1)	2.65(1)	9.78(1)	2.74(1)
170	7.70(1)	3.69(1)	1.37(2)	4.04(1)
160	1.02(2)	4.90(1)	1.83(2)	5.79(1)
150	1.25(2)	6.05(1)	2.28(2)	8.03(1)
140	1.42(2)	6.95(1)	2.66(2)	1.07(2)
130	1.52(2)	7.50(1)	2.96(2)	1.35(2)
120	1.70(2)	8.50(1)	3.40(2)	1.63(2)

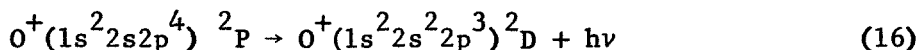
3. EXCITATION REMOVAL PROCESSES

3.1 Atomic Oxygen Ions

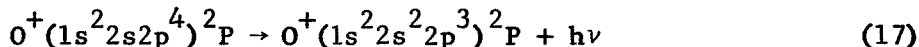
The excited $O^+ 4P$ state produced by (4) will decay rapidly according to the allowed transition



with the emission of a photon of wavelength 8446\AA which can be absorbed by atomic and molecular oxygen in the transitions (1) and (10) respectively. The excited state produced by (5) will also decay rapidly either through



with the emission of a photon of wavelength 8446\AA or through



with the emission of a photon of wavelength 8446\AA . According to Cohen and Dalgarno [15], the relative probability of occurrence of (16) to (17) is 3.27. In both cases, the emitted photon produces further ionization and the rates of population of the metastable states of O^+ are slightly increased by the cascade processes.

The radiative lifetime of the $2D_{3/2}$ metastable state of O^+ is 5×10^3 sec and of the $2D_{5/2}$ state, 2×10^4 , [16]. They can be deactivated by electron impact



the rate coefficient of which is about $3 \times 10^{-8} \text{cm}^3 \text{sec}^{-1}$ [16] or by collisions with neutral particles such as ion-atom interchange



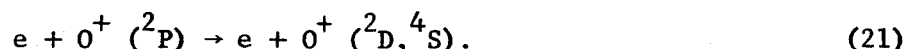
and charge transfer



Omholt [17] has pointed out that if the N_2^+ ion in (20) is produced in the $v = 1$ vibrational level of the $A^2\pi_u$ state, the process is in close resonance and Hunten [18] has presented evidence that the 1-0 and 1-2 bands of the Meinel system may often have anomalously high intensities during auroras. The $O^+(2D-4S)$ multiplet at $\lambda\lambda 3729-3726$ has been observed in auroras by several groups (cf. Chamberlain [19]). It is variable in occurrence and was not positively identified until the great red aurora of February 11th, 1958 when Wallace [20] resolved the two lines. Its weakness in ordinary

auroras suggests that deactivation is severe and there seems little possibility that significant radiation can occur in the normal dayglow. However, if (20) is responsible for suppressing the emission there may occur an enhancement of the $v' = 1$ progression of the Meinel band system, a possibility to which we shall return in Section 4.

The radiative lifetime of the $^2P_{1/2}$ metastable state is 5 sec and of the $^2P_{3/2}$ metastable state 4 sec and significant radiation may arise from the 2P states [1], the computed overhead intensity at noon in the absence of deactivation being 1.5 kilorayleighs. The 2P states will undergo some deactivation by impacts with the ambient electrons



We adopt the electron density distribution listed in Table 1 and a rate coefficient α for (21) of $1 \times 10^{-7} \text{ cm}^3 \text{ sec}^{-1}$ [16]. The effect of electron impact deactivation on the luminosity altitude profile of radiation emitted by $O^+ (^2P)$ is shown in Figure 1. Electron impact deactivation reduces the overhead intensity from 1.5 to 1.3 kilorayleighs.

The $^2P-^2D$ multiplet at $\lambda\lambda 7319-7330$ has been observed in auroras [17,20,21] and Chamberlain [19] has argued that the observations indicate some deactivation, occurring presumably through reactions similar to (19) and (20). The effects of a deactivation coefficient of $10^{-10} \text{ cm}^3 \text{ sec}^{-1}$ in collisions with N_2 on the altitude profiles of radiation emitted from the 2P states are illustrated in Figure 1. The emission at low altitudes is suppressed and the peak intensity occurs at 200 km instead of 150 km. The overhead intensity is reduced from 1.3 to 0.5 kilorayleighs.

Because of the uncertainty in the deactivation coefficient, accurate predictions of the intensities of the four lines of the $^2P-^2D$ multiplet are not possible. The intensities given in Table 5 correspond to no deactivation by N_2 and to a deactivation coefficient of $10^{-10} \text{ cm}^3 \text{ sec}^{-1}$. They are consistent with an earlier estimate [1].

3.2 Molecular Nitrogen Ions

The excited $N_2^+ (^2\Sigma_u^+)$ molecules produced by (9) will, if stable, decay rapidly to the $B^2\Sigma_u^+$ and $A^2\pi_u$ states. The resulting emission is concentrated in the ultraviolet region of the spectrum and it will be reabsorbed by O_2 and O_3 . We assume arbitrarily that the cascading is primarily to the $A^2\pi_u$ state in which case its population is increased by about 12%.

The $A^2\pi_u$ and $B^2\Sigma_u^+$ states both decay rapidly by allowed transitions giving rise respectively to the infra-red Meinel system and the first negative system. Deactivation is unimportant and the rates of population shown in Figure 2 are also the rates of emission of the two systems. The overhead

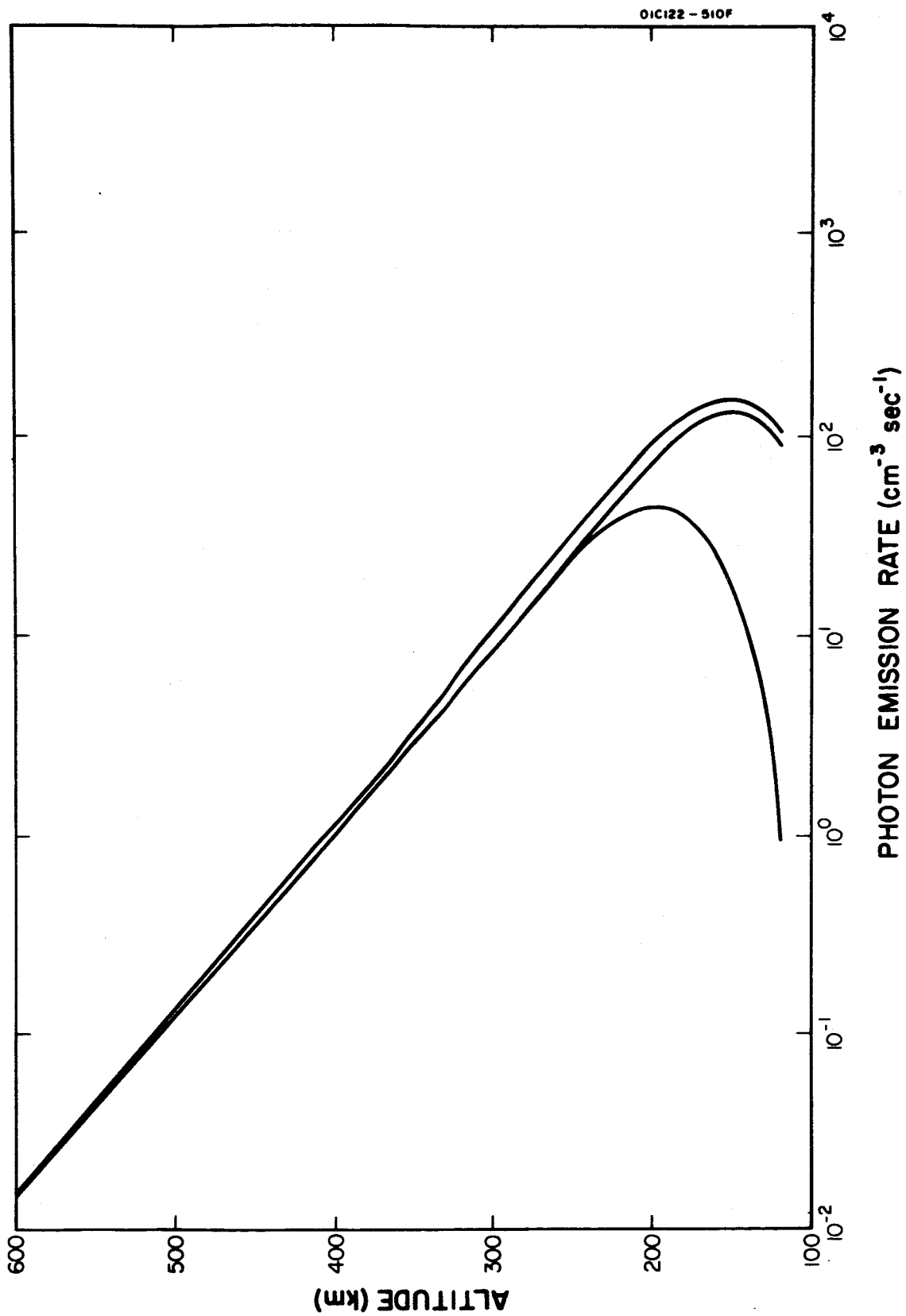


Figure 1. The altitude profile of fluorescent emission at noon from the $\text{O}^+(\text{P-}^2\text{D})$ transition. From right to left, the curves show the inclusion of electron impact deactivation and molecular nitrogen impact deactivation.

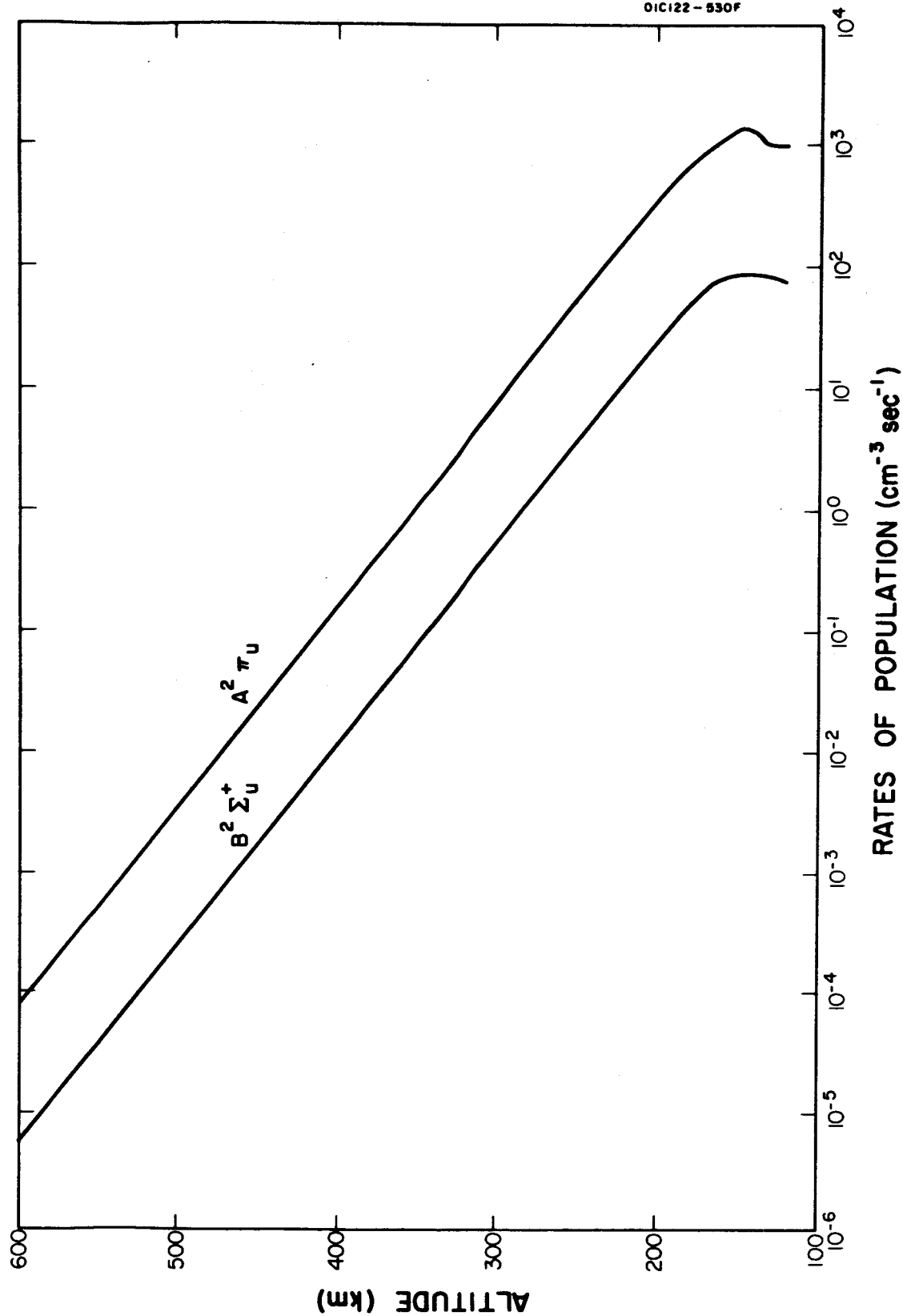


Figure 2. The rates of population at noon of the upper levels $A^2 \pi_u$ and $B^2 \Sigma_u^+$ of respectively the Meinel and the first negative band systems of nitrogen.

TABLE 5
 INTENSITIES AT NOON OF THE $O^+(^2P - ^2D)$ LINES

Transition	Wavelength (Å)	Intensity in Rayleighs	
		No Deactivation	N ₂ Deactivation
$^2P_{1/2} - ^2D_{3/2}$	7329.9	280	100
$^2P_{1/2} - ^2D_{5/2}$	7318.6	190	70
$^2P_{3/2} - ^2D_{3/2}$	7330.7	280	120
$^2P_{3/2} - ^2D_{5/2}$	7319.4	520	230

intensities are shown as functions of altitude in Figure 3. Above 120 km the intensity of the Meinel system is 9 kR and the intensity of the first negative system is 600 R.

It is not possible to predict with confidence the distributions of intensities within the band systems because a significant contribution to photoionization may come from autoionizing processes [7] which do not necessarily conform to the Franck-Condon principle. If autoionization is not important the vibrational distributions are governed mainly by the Franck-Condon factors [22] and the intensity distribution in the first negative system should approximate that of Table 6. The intensity distribution in the Meinel system is less well determined but perhaps 3 kR will appear in the (2,0) band at 7850\AA , 1.5 kR in the (3,1) band at 8080\AA , and 750 R in the (4,2) band at 8321\AA .

3.3 Molecular Oxygen Ions

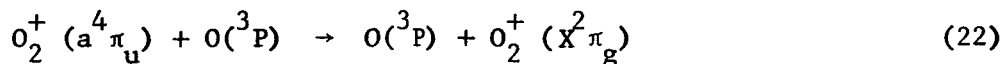
The unidentified doublet and quartet states of O_2^+ will decay rapidly by allowed transitions in the ultraviolet or they may dissociate into O and O^+ . The cascading transitions will increase the populations of the lower lying levels of O_2^+ but in no case will the increase exceed 10% and we exclude the high lying states from further consideration.

The $c^4\Sigma^-$ and $b^4\Sigma^-$ states produced respectively by (14) and (13) will radiate by allowed transitions. The former gives rise to the Hopfield emission bands $c^4\Sigma^- - b^4\Sigma^-$ in the ultraviolet [23] and the latter to the first negative band system $b^4\Sigma^- - a^4\pi_u$ in the region of 6000\AA . Deactivation is unimportant and the rates of population shown in Figure 4 are also the rates of emission of the two systems. The overhead intensities are shown as functions of altitude in Figure 5. Above 120 km, the intensity of the Hopfield emission bands is 600 R and of the first negative system 2 kR.

The vibrational distribution in the first negative system which occurs if the Franck-Condon principle is applicable (see however [7]) is given in Table 7.

The $A^2\pi_u$ state produced by (12) decays to the ground state with the emission of the second negative band system in the ultraviolet. The luminosity profile is illustrated in Figure 4 and the overhead intensity in Figure 5. Above 120 km the overhead intensity is 420 R.

The $a^4\pi_u$ state produced by (11) and by cascading from the $b^4\Sigma^-$ state is metastable. It is probably severely deactivated by electron impacts and by collision processes such as atom-atom interchange



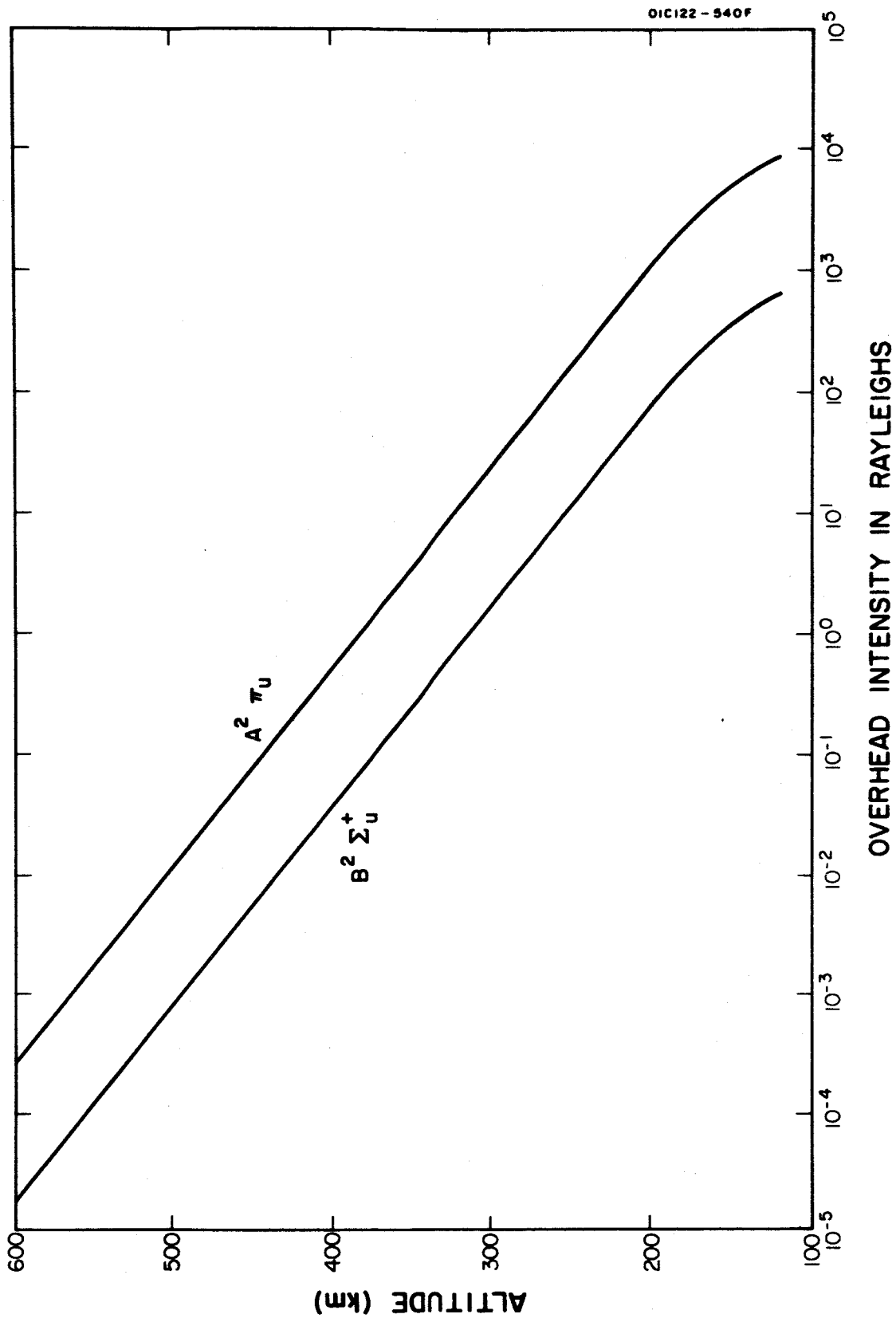


Figure 3. The overhead intensities of the Meinel and first negative band systems of nitrogen.

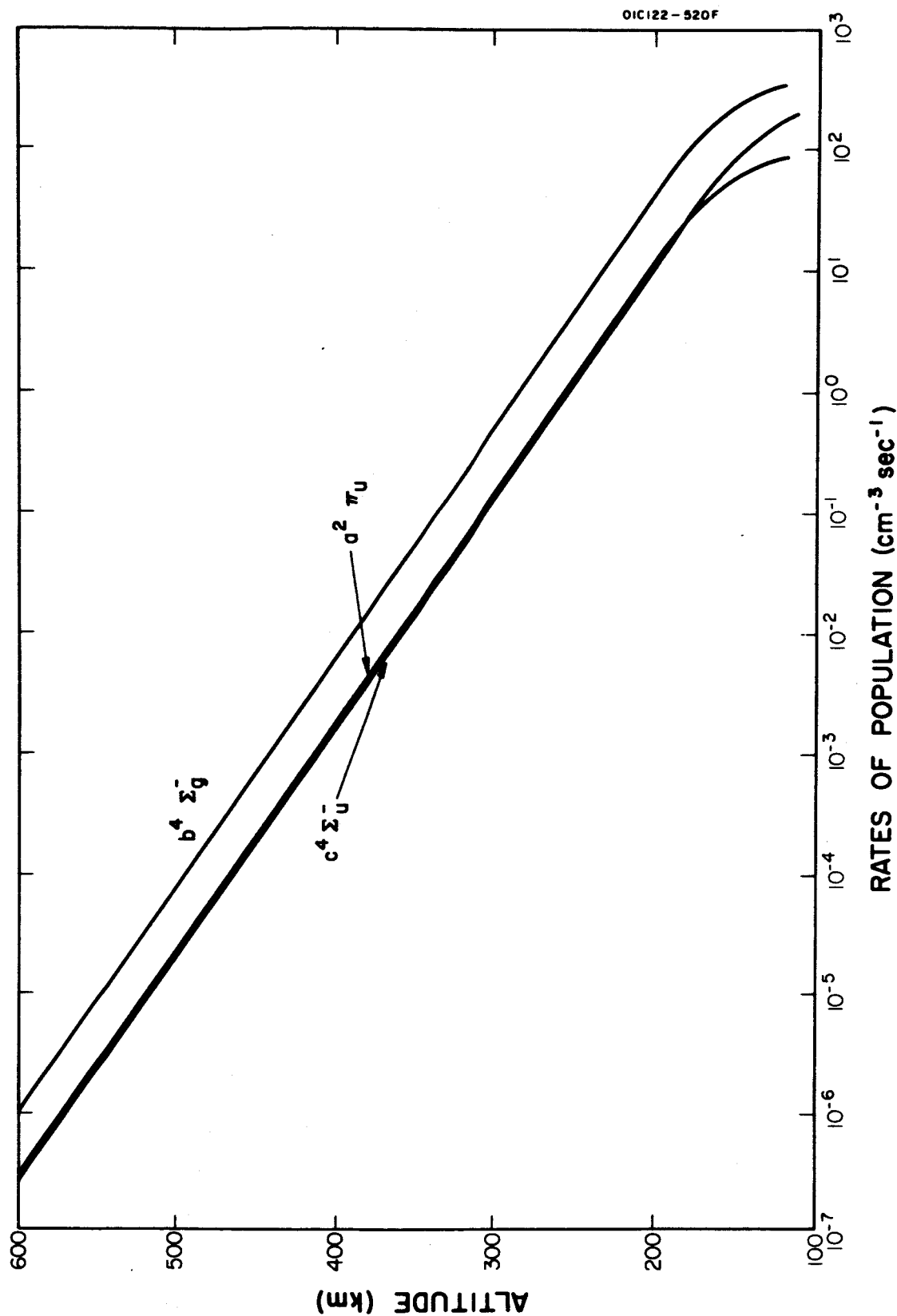


Figure 4. The rates of population at noon of the upper levels $c^4 \Sigma_u^-$, $b^4 \Sigma_g^-$ and $A^2 \pi_u$ of, respectively, the Hopfield and the first and second negative band systems of oxygen.

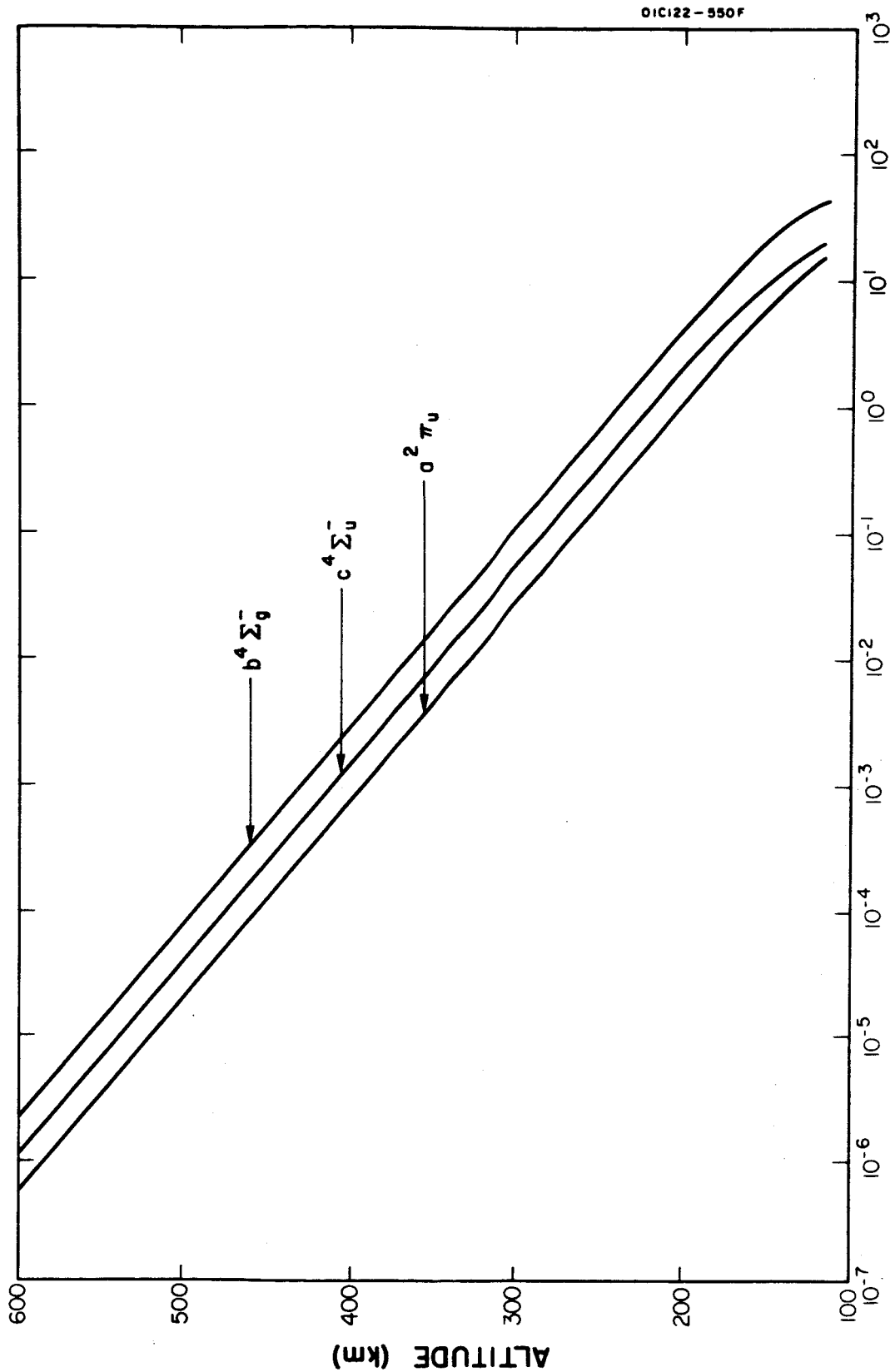


Figure 5. From right to left the curves show the overhead intensities of the first negative, the Hopfield and the second negative systems of oxygen.

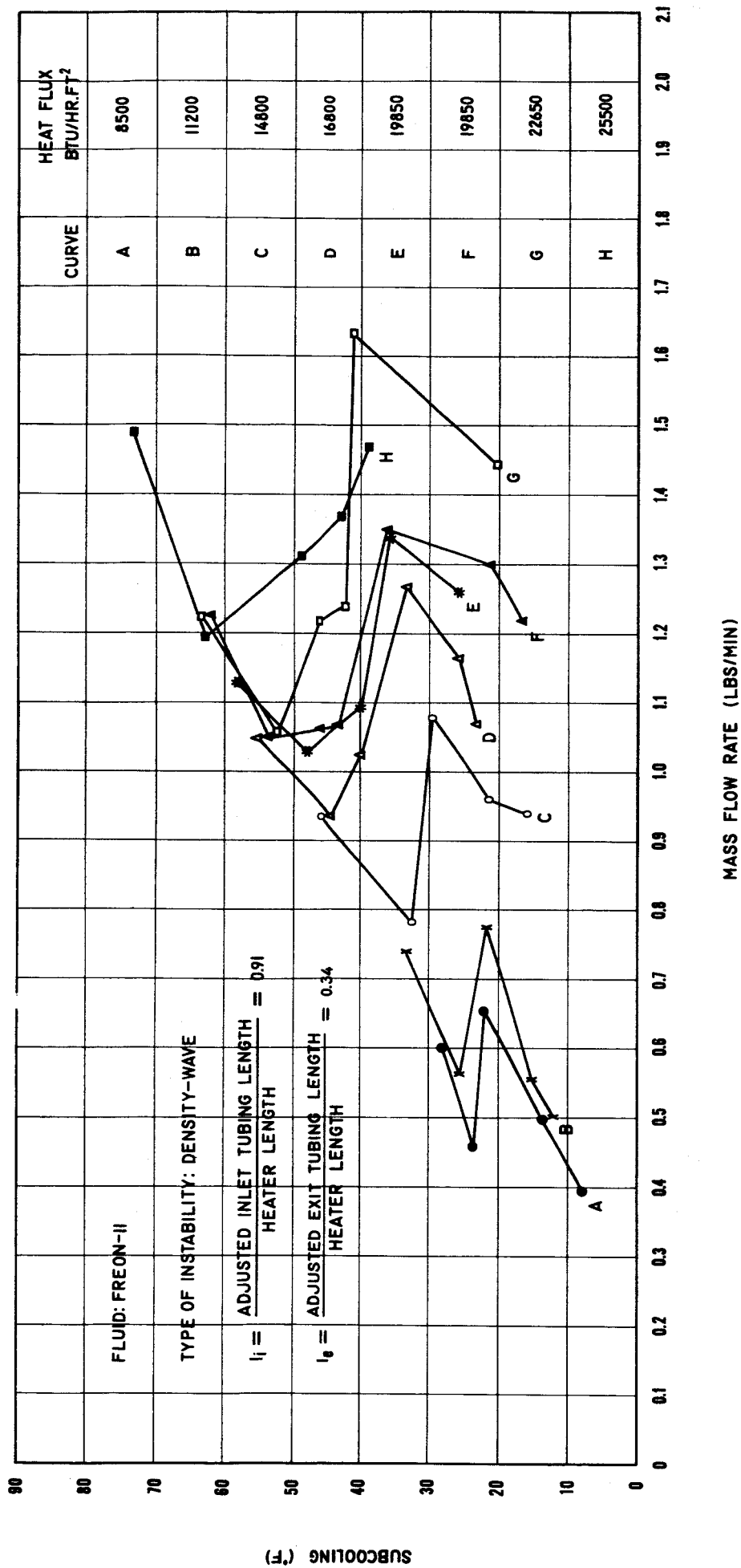


FIG. 6.- SUBCOOLING VS MASS FLOW RATE AT STABILITY BOUNDARY FOR FIXED GEOMETRY (NO EXIT VALVE)

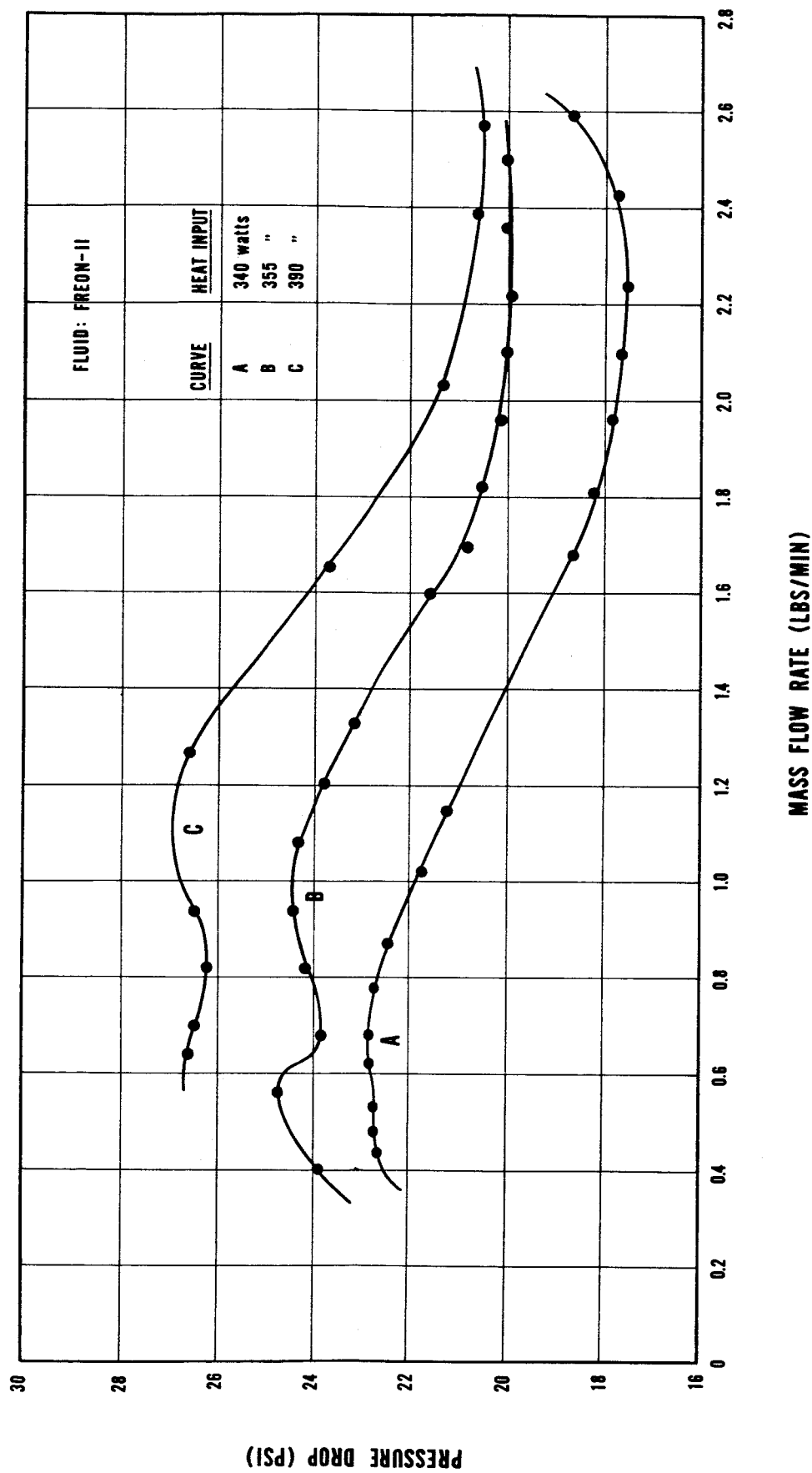


FIG. 7.— STEADY STATE BOILING FLOW PRESSURE DROP VS MASS FLOW RATE RELATIONSHIPS

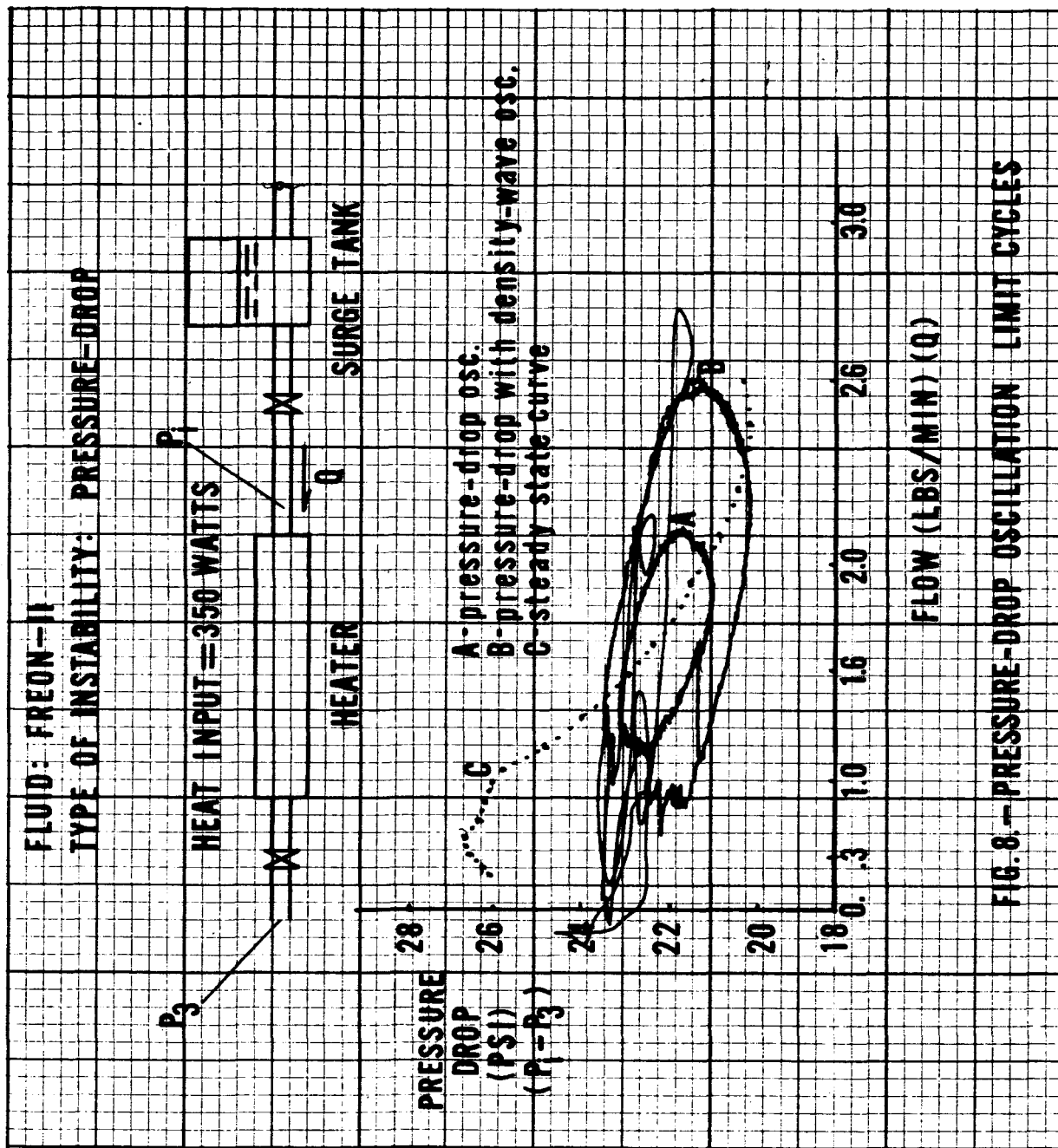


TABLE 6
OVERHEAD INTENSITIES AT 120 KM OF THE FIRST NEGATIVE SYSTEM OF N_2^+
DUE TO FLUORESCENCE

Band	Wavelength (Å)	Intensity (Rayleighs)
0,0	3914.4	720
0,1	4278.1	100
0,2	4709.2	25
0,3	5228.3	5
1,0	3582.1	25
1,1	3884.3	20
1,2	4236.5	20
1,3	4651.8	15
1,4	4148.8	2

TABLE 7
OVERHEAD INTENSITIES AT 120 KM OF THE FIRST NEGATIVE SYSTEM OF O_2^+

Band	Wavelength (Å)	Intensity (Rayleighs)
0,0	6026	180
0,1	6419	200
0,2	6856	150
1,0	5632	420
1,1	5973	30
1,2	6351	45
2,0	5296	75
2,1	5598	60
2,2	5926	45

and little emission is to be expected. With our (arbitrary) assumptions about the individual photoionization cross sections, the integrated rate of production of metastable molecules above 120 km is $1.5 \times 10^9 \text{ cm}^{-2} \text{ sec}^{-1}$ compared to a total O_2^+ production rate of $1.3 \times 10^{10} \text{ cm}^{-2} \text{ sec}^{-1}$. Accordingly metastable $a^4\pi_u \text{O}_2^+$ molecules may play a significant role in determining ionospheric composition in the E and lower F regions.

4. OTHER EXCITATION MECHANISMS

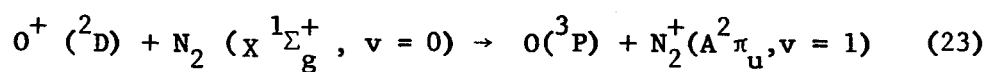
The excited ionic states may be populated by other mechanisms in addition to the direct absorption of solar radiation. Collisions between the fast photoelectrons produced by photoionization and the neutral atmospheric particles constitute a source of excitation which may be significant. Detailed calculations will be required in general but an estimate of the electron impact contribution to the first negative system of nitrogen can be readily obtained using the known efficiency with which electrons absorbed in air produce 3914Å emission (cf. Dalgarno [24]). Electron impacts are responsible for about 450 R above 120 km. It may be shown that as in auroras (cf. Chamberlain [19]) electron impact with the positive ions gives a negligible contribution despite the large threshold cross sections.

Resonance scattering of solar radiation by the positive ions must be a major source of excitation if the upper state is accessible by an allowed transition from the ground state. Thus resonance scattering by N_2^+ ground state ions contributes to the N_2^+ first negative and Meinel band systems and resonance scattering by O_2^+ ground state ions contributes to the O_2^+ second negative system. Resonance scattering by O_2^+ a $^4\pi_u$ metastable molecules may contribute to the O_2^+ first negative system.

The 0-0 band at 3914Å has been observed in the day airglow by Wallace and Nidey [25] and by Zipf and Fastie [26], who have shown that with plausible assumptions about the N_2^+ density distribution the measured intensities of 5 kR at a solar zenith angle of 76° [25] and of 7 kR at a solar zenith angle of 60° [25] can be explained by resonance scattering. The predicted intensity from fluorescent scattering and from electron impact is several hundred rayleighs for the solar angles obtaining during the measurements but their contributions are detectable in principle by a detailed analysis of the luminosity profile low in the atmosphere where there are few N_2^+ ions and by the Swings effect (cf. [27], [25]).

Zipf and Fastie [26] have concluded from their observations that the efficiency with which photoionization of nitrogen produces a 3914Å photon is at most 5%. Our predictions at 120 km, based on Schoen's data [7] and assuming no contribution by downward transitions from the $^2\Sigma^+$ state, are equivalent to an efficiency of 2.7% for photoionization and an efficiency of 3.7% for the associated electron impact ionization. The uncertainties in the composition of the neutral atmosphere are such that there is not necessarily any discrepancy.

Specific collision processes by which an ion is converted into a different species may lead to selective enhancements of spectral features. Only one appears to be of interest for ionic emissions. If all the $O^+(^2D)$ ions were removed by



4 kR of radiation would occur in the Meinel bands originating in the $v = 1$ level, comparable to that anticipated from fluorescence. The altitude distributions of the two sources would differ significantly, fluorescence tending to follow the nitrogen distribution and (23) tending to follow the oxygen distribution.

REFERENCES

1. A. Dalgarno and M. B. McElroy, Planetary Space Sci., 11, 727, (1963).
2. A. Dalgarno, R. J. W. Henry and A. L. Stewart, Planetary Space Sci., 12, 235, (1964).
3. A. Dalgarno, M. B. McElroy and R. J. Moffett, Planetary Space Sci., 11, 463, (1963).
4. R. E. Huffman, Y. Tanaka and J. C. Larrabee, Disc. Faraday Soc., 37, 159, (1964).
5. G. R. Cook, B. K. Ching and R. A. Becker, Disc. Faraday Soc., 37, 149, (1964).
6. J. A. R. Samson and R. B. Cairns, J. Geophys. Res., 69, 4583, (1964).
7. R. I. Schoen, J. Chem. Phys. 40, 1830 (1964).
8. D. R. Bates, Proc. Roy. Soc. A253, 451 (1959).
9. M. B. McElroy, Contribution from the Kitt Peak National Observatory, No. 55 (1964).
10. H. E. Hinteregger, L. A. Hall and G. Schmidtke, Space Science V, Ed. P. Muller (North-Holland:Amsterdam) (1965).
11. M. B. McElroy, Planetary Space Sci., 13, 403 (1965).
12. H. E. Hinteregger, J. Geophys. Res. 66, 2367 (1961).
13. L. A. Hall, W. Schweizer and H. E. Hinteregger, J. Geophys. Res., 70, 105 (1965).
14. L. A. Hall, W. Schweizer, L. Heroux and H. E. Hinteregger, Astrophys. J., (1965).
15. M. Cohen and A. Dalgarno, Proc. Roy. Soc. A280, 258 (1964).
16. M. J. Seaton and D. E. Osterbrock, Astrophys. J., 125, 66 (1957).
17. A. Omholt, J. Atmos. Terr. Phys. 10, 324, (1957).
18. D. M. Hunten, Annales de Geophys. 14, 167 (1958).

REFERENCES (Continued)

19. J. W. Chamberlain, Physics of the Aurora and Airglow, (Academic Press: New York) 1961.
20. L. Wallace, J. Atmos. Terrest. Phys. 17, 46 (1959).
21. M. Dufay, Ann. Geophys. 15, 134 (1959): A. Vallance Jones, Can. J. Phys. 38, 453 (1960).
22. R. W. Nicholls, Annales de Geophys. 20, 99 (1964).
23. F. J. LeBlanc, J. Chem. Phys. 38, 487 (1963).
24. A. Dalgarno, Annales de Geophys. 20, 67 (1964).
25. L. Wallace and R. A. Nidey, J. Geophys. Res. 69, 471 (1964).
26. E. C. Zipf and W. G. Fastie, J. Geophys. Res. 69, 2357, (1964).
27. A. Vallance Jones and D. M. Hunten, Can. J. Phys. 38, 458 (1960).